Distribution and transportation of Fukushima-derived radiocesiums in the seawater of the Northwest Pacific ocean in May 2013

Fenfen Wang [a], Wu Men [c,*], Jiang Huang [a], Zhaohui Chen [b], Lixiao Xu [b]

[a] The Laboratory of Marine Ecological and Environmental Early Warning and Monitoring, Third Institute of Oceanography, Ministry of Natural Resources, 184 Daxue Road, Xiamen, 361005, China
[b] Qingdao National Laboratory for Marine Science and Technology, Qingdao, 266237, China
[c] School of Marine Sciences, Nanjing University of Information Science and Technology, Nanjing, 210044, China

HIGHLIGHTS

- More FDNPP Cs were transported to subtropical area by STMW in 2013.
- The FDNPP-derived Cs mainly existed in the upper 500 m of water column.
- No FDNPP-derived Cs was found below 1000 m layer.
- The low salinity water restrained the deeper penetration of FDNPP Cs.
- Cyclonic eddy promoted more Cs deeper penetration besides the subduction of STMW.

GRAPHICAL ABSTRACT
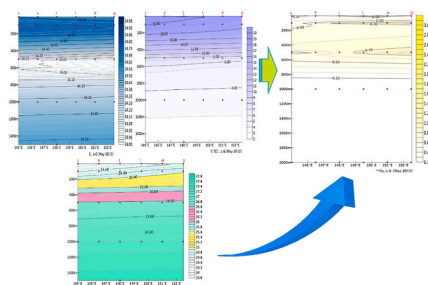
ARTICLE INFO

ABSTRACT

The Fukushima Daiichi Nuclear Power Plant (FDNPP) has generated quantities of polluted water since the accident in 2011 triggered by the massive earthquake. In order to understand the FDNPP accident comprehensively and to provide a basic reference for predicting the transport of the treated nuclear contaminated water in the Northwest Pacific further, the distributions of ^{137}Cs and ^{134}Cs in the seawater as deep as 2000 m were determined in the subtropical region in May 2013. The results suggested that the radiocesium from FDNPP still existed in May 2013. But no FDNPP-derived radiocesium was found below 1000 m layer. The FDNPP accident contributed 0.46 PBq of ^{137}Cs to the upper 500 m of water column, which was ~1.6 times of the background amount of ^{137}Cs (0.28 PBq). The maximum activities of ^{137}Cs and ^{134}Cs were 7.88 Bq/m^3 and 3.40 Bq/m^3, respectively. It is mainly because of the Subtropical Mode Water (STMW) that carried ^{137}Cs and ^{134}Cs to the subtropical region along the subsurface isopycnals (25.0–25.6 δ_θ). As time went on, more FDNPP-derived radiocesiums were transported to the subtropical region and to the subsurface layer by the STMW than ever. The cyclonic mesoscale eddy further promoted more radiocesiums downward transport and deeper penetration on the basis of the subduction of STMW. However, the formation of the vertical stratification and the presence of the low salinity water mass (at the depth of ~500–~700 m) restrained the penetration of the radiocesium into deeper and interior ocean and thus the FDNPP-derived ^{137}Cs and ^{134}Cs in the subtropical area mainly distributed in the upper 500 m layer.

* Corresponding author.
  E-mail address: menwu@nuist.edu.cn (W. Men).

1. Introduction

On March 11, the Fukushima Daiichi Nuclear Power Plant (FDNPP) accident occurred and great amounts of radioactive pollutants were released into the environment, of which ~80% entered into the North-west Pacific (Christoudias and Lelieveld, 2013; Yoshida and Kanda, 2012; Lin et al., 2015). Over the past 12 years, the subsequent leakage, pollution, impact and countermeasures of the accident have been continuously reported, which aroused the public's concern every time. Although the disposal has been implemented for almost 12 years, it will take another 20–30 years to complete the entire decommissioning process of the damaged unit 1–4 in the FDNPP (METI, 2022). At present, Japanese government plans to discharge the nuclear contaminated water (NCW) into the sea area 1 km away from the FDNPP through a submarine tunnel in 2023 after using an Advanced Liquid Processing System (ALPS) to remove most of the pollutants (TEPCO, 2021). It causes the public's great concerns again. The NCW is treated by the ALPS and stored in more than 1000 tanks. As of Mar. 16, 2023, total amount of the treated water is up to 1,328,181 m^3, and will reach the maximum capacity of 1.37 million m^3 soon (TEPCO, 2021). Therefore, how the discharged NCW transported as well as its resulting impact will be are the most concerned issue currently. So far, the distributions of ^{134}Cs and ^{137}Cs in the North Pacific have been extensively determined to investigate the influence of FDNPP on the marine environment and to study the dispersion patterns of the FDNPP pollutants, including transportation of radiocesium measured or simulated by models. (Kumamoto et al., 2014, 2013, 2019; Kaeriyama et al., 2014, 2016, 2017; Aoyama et al., 2013a,b, 2016a,b; Men et al., 2015; Men, 2021; Buesseler et al., 2017; Wang et al., 2022a; Inomata et al., 2018; Takata et al., 2018;

Inoue et al., 2012; Nakata and Sugisaki, 2015). However, the southward dispersion of FDNPP-derived radioactive Cs reported was mainly about the distributions during 2011 and 2012 (Kaeriyama et al., 2014, 2016; Kumamoto et al., 2014, 2015). The vertical distributions of the ^{134}Cs and ^{137}Cs in the seawater in May 2013 in the south of Kuroshio Extension (KE) area of Northwest Pacific are quite rare, especially for the depth as deep as 2000 m. In order to understand the impact of the FDNPP comprehensively, the activities, distributions and transport of ^{134}Cs and ^{137}Cs as deep as 2000 m in May 2013 was measured in the Subtropical area in this work, aiming to provide a comprehensive image for the transport of FDNPP-derived radiocesiums and a basic reference for predicting the transport of the discharged NCW in the Northwest Pacific.

2. Materials and methods

2.1. Sampling stations

The sampling stations are shown in Fig. 1. The study areas were located in the Northwest Pacific subtropical area to the southeast of Japan (145.01–152.51°E, 26.99–33.00°N). Seawater samples were vertically sampled from 21 stations in May 2013. The sampling depths ranged as deep as 2000 m. The additional details of the sampling station are shown in Table A1 in Appendix data.

2.2. Sampling method and analysis method

60 L seawater sample were collected at each depth by a CTD-rosette assembly with Niskin bottle samplers (Model Sea-Bird 911plus, Sea bird electronics, Inc., Bellevue, Washington, USA) and stored in polyethylene
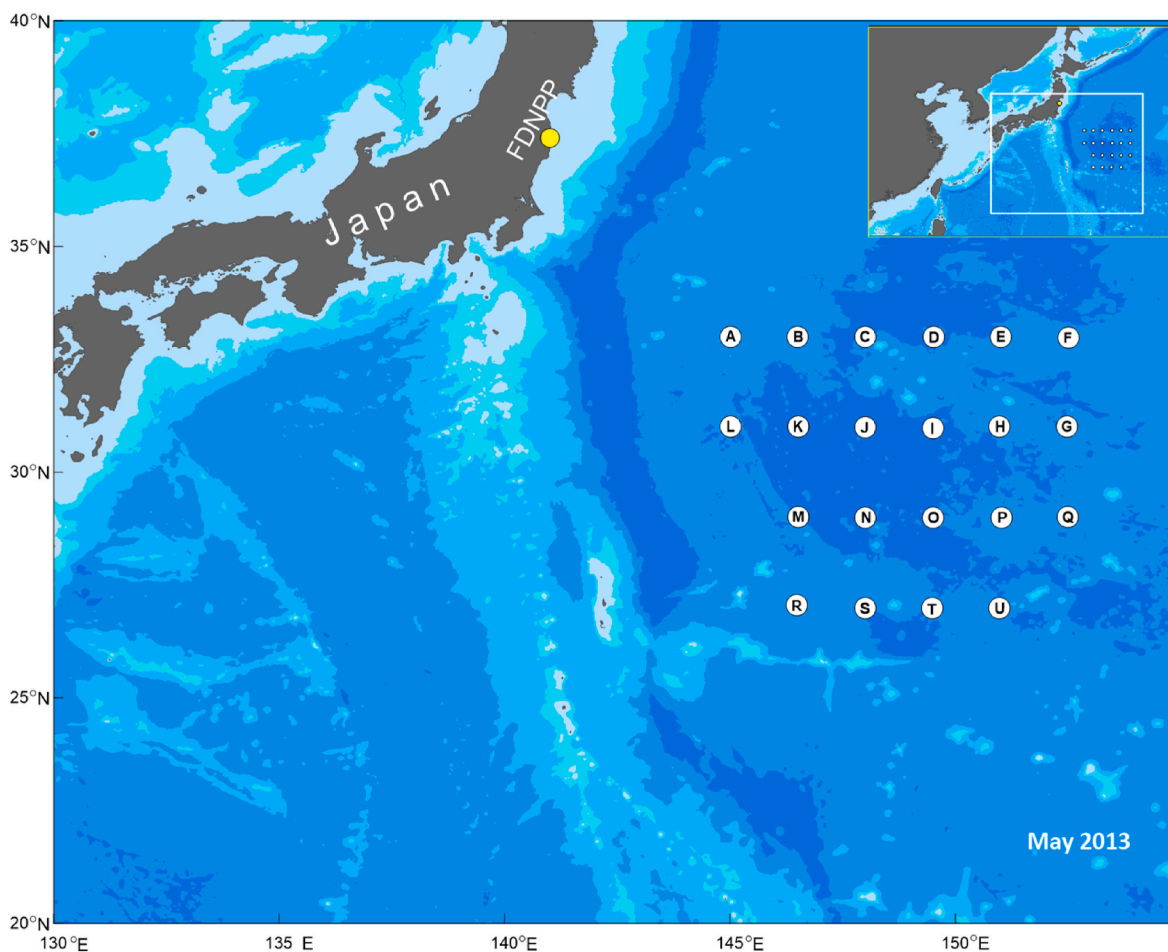

Fig. 1. Map of sampling stations.

barrels with acidification (pH ~2). The AMP (ammonium phosphomolybdate) coprecipitation and γ spectrometry detection were employed to determine the activities of ^{134}Cs and ^{137}Cs (Wang et al., 2022a). Briefly, 30 mg CsCl were added as chemical yield tracer, followed by 18 g AMP to be co-precipitated. 30-minute stirring made the AMP and CsCl well mixed with the seawater sample and more than 24-h standing allowed the AMP-Cs coprecipitation well settled. Remove the supernatants by siphoning and filter the residual. Put the filter into a muffle and heat for 2 h under 450 °C. After cooling down, measure the residue using the HPGe γ spectrometer to determine the activities of ^{134}Cs and ^{137}Cs. ^{137}Cs (LEA ^{137}Cs standard CS137EGSA10) and ^{134}Cs (PTB ^{134}Cs standard 2011–1622) standard solution were used for the efficiency calibration. The Minimum Detectable Activity (MDA) for ^{137}Cs and ^{134}Cs were 0.21 Bq/m^3 (661.7 keV) and 0.20 (604.7 keV) Bq/m^3, respectively.

3. Results

The activities of ^{137}Cs and ^{134}Cs in the seawater column in the Northwest Pacific in May 2013 are shown in Table A1 Ap pendix data. The activities of ^{137}Cs and ^{134}Cs in the surface seawater ranged from 1.63 ± 0.19 to 4.09 ± 0.33 Bq/m^3 and < MDA to 1.19 ± 0.11 Bq/m^3, respectively. At the depth of 100 m, ^{137}Cs ranged from 1.80 ± 0.22 to 7.88 ± 0.58 Bq/m^3 and ^{134}Cs was in the range of < MDA - 3.40 ± 0.29 Bq/m^3. The station Q had the highest ^{137}Cs and ^{134}Cs activities. At the depth of 500 m, ^{137}Cs and ^{134}Cs were in the ranges of 1.01 ± 0.13–5.20 ± 0.52 Bq/m^3 and < MDA - 2.38 ± 0.29 Bq/m^3, respectively. At the depth of 1000 m, ^{137}Cs ranged from < MDA to 0.76 ± 0.11 Bq/m^3 and ^{134}Cs was < MDA. At the depth of 2000 m, both ^{137}Cs and ^{134}Cs were < MDA.

4. Discussion

4.1. The contributions of FDNPP accident to the radiocesium in subtropical area

Before the FDNPP accident, radiocesiums in the Northwest Pacific Ocean were mainly originated from the atmosphere nuclear weapons testing in 1950s–1980s through the global stratospheric fallout and the PPG (Pacific Proving Ground) close-in fallout. Due to the short half-life of 2.06 years, ^{134}Cs from the global fallout and close-in fallout has almost disappeared. Thus, ^{134}Cs is a valuable indicator of FDNPP-derived cesium and all of the ^{134}Cs in the seawater of the study area were thought to be derived from FDNPP accident. ^{137}Cs, unlike ^{134}Cs, could stay in the ocean for more than one hundred years because of its longer half-life of 30.07 years. Therefore, ^{137}Cs in the North Pacific Ocean was dominantly attributed to the global fallout and PPG close-in fallout, which inventory was 104 PBq (Kaeriyama, 2017; Buesseler, 2014). The FDNPP accident released additional 15–20 PBq of ^{137}Cs or ^{134}Cs into the North Pacific Ocean and the typical characteristic activity ratio of ^{134}Cs/^{137}Cs for Fukushima accident at the time of accident was ~1 (Aoyama et al., 2016a, b; Kaeriyama, 2017; Buesseler et al., 2017; Men et al., 2015). Therefore, based on ^{134}Cs/^{137}Cs$_{activity\ ratio} \approx 1$, the FDNPP-derived ^{137}Cs can be estimated by decay-correcting ^{134}Cs to the time of the accident. Then the activity of ^{137}Cs derived from the fallout (global and close-in fallout) were the difference between the measured ^{137}Cs activity and the FDNPP-derived ^{137}Cs activity. According to Table A1 in the Appendix data, the activity level of the fallout-derived ^{137}Cs in the study area before FDNPP accident was obtained to be < 1.98 Bq/m^3, which is consistent with the reported ^{137}Cs background level before FDNPP accident in the North Pacific (<2 Bq/m^3) (Kaeriyama, 2017; Men, 2021). All the ^{137}Cs and ^{134}Cs data with their corresponding depth were plotted in Figure A1 Ap pendix data. It shows that the majority of the ^{137}Cs and ^{134}Cs distributed in the upper 500 m of the water column. The highest ^{137}Cs activity (7.88 Bq/m^3) was almost ~4 times of the background level. The average ^{137}Cs activities in the upper 500 m of water column were 3.00 Bq/m^3, obviously higher than

the background level. The highest ^{134}Cs activity was 3.40 Bq/m^3 with the average of 0.76 Bq/m^3. It reflected that the study area was still polluted by FDNPP accident. The contributions of FDNPP accident to the ^{137}Cs activity concentrations in different layers of the seawater columns were estimated and listed in the last column of Table A1 in Appendix data. It exhibited that FDNPP accident contributed ~53.5% of the ^{137}Cs to the upper 500 m of water column in average. Correspondingly, the global and close-in fallout contribution was ~46.5% (1 minus 53.5%).

4.2. The temporal distribution of the ^{137}Cs and ^{134}Cs

In Dec. 2011 (9 months after FDNPP accident) in Wang et al. (2022b), there was only a little Fukushima-derived radiocesium transported across the Kuroshio Extension (KE) to the subtropical area, compared with the activities of radiocesium in the north of the KE area. It was attributed that the KE formed a southern boundary for the transport of the FDNPP-derived radiocesium, reported in the previous reports (Buesseler et al., 2012; Kumamoto et al., 2014). However, according to the variations of the ^{134}Cs activities at the different depths from Dec. 2011 to May 2013 shown in Table A2 in Appendix data and Fig. 2, the average ^{134}Cs activities increased apparently in surface and 100 m layer in May 2013 relative to those in 2012 during the range of this study area (26°N to 33°N, 145°E to 152°E) (Kumamoto et al., 2015; Kaeriyama et al., 2016; Deng et al., 2020). Especially, if the decay of ^{134}Cs is considered further, it means and reflects that more FDNPP-derived radiocesiums had been transported to the south of KE with time elapsed in May 2013.

In addition, as shown in Table A2 and Fig. 2, for the depth of 100 m, the highest ^{134}Cs activities were observed and both the highest and average ^{134}Cs activities showed a significant increase from Dec. 2012 to May 2013, ranging from 0.70 to 3.40 Bq/m^3 and 0.24–1.23 Bq/m^3, respectively. The water potential density of this subsurface ^{134}Cs maximum (100 m) ranged 25.0–25.6 kg/m^3, which corresponds to that of STMW (100 m–300 m). STMW is a water mass characterized by vertical homogeneity of temperature and density in the upper thermocline (a thermostad or pycnostad) in subtropical area (Suga and Hanawa, 1990). It formed in the surface mixed layer in winter by strong winter ventilation in the region south of the Kuroshio Extension, then subducted and advected southeastward along the subtropical gyre (Hanawa and Yoritaka, 2001). Therefore, it is indicated that more FDNPP-derived radiocesiums were transported and subducted to the subsurface layer by STMW than ever.

Besides, the highest ^{134}Cs activities in 500 m layer in May 2013 have also increased apparently than those in Jan. 2012 (Table A2) despite of more or less the same with those in Oct. 2012 and Dec. 2012. Suga and Hanawa (1990) presented the seasonal variation of the mixed layer in the northwestern North Pacific Subtropical gyre and the formation area of Subtropical Mode Water and showed the mixed layer deepening remarkably in wintertime. Thus, the variation of ^{134}Cs was associated with the seasonal variation of the Subtropical Mode Water mixed layer to a certain extent. Even so, the activities of ^{134}Cs in 500 m layer in 2012 were still lower than those in May 2013 after the ^{134}Cs decay corrected. Therefore, it illustrated that more FDNPP-derived radiocesiums were transported and subducted to the deeper layer into marine interior than ever with time elapsed.

4.3. The spatial distributions of ^{137}Cs and ^{134}Cs

The horizontal distributions of ^{137}Cs and ^{134}Cs at the depths of 3 m, 100 m, 500 m and 1000 m were shown in Fig. 3. The distributions of ^{137}Cs were similar to those of ^{134}Cs. The distributions at different depths differed from each other. In Figs. 3 and 2, for the surface layer, the ^{137}Cs and ^{134}Cs activities at each longitude decreased gradually from 33°N to 26°N. For the subsurface layer (100 m), the ^{137}Cs and ^{134}Cs activities at each longitude varied little with latitude except the southernmost section. It was mainly associated with the formation and subduction of the
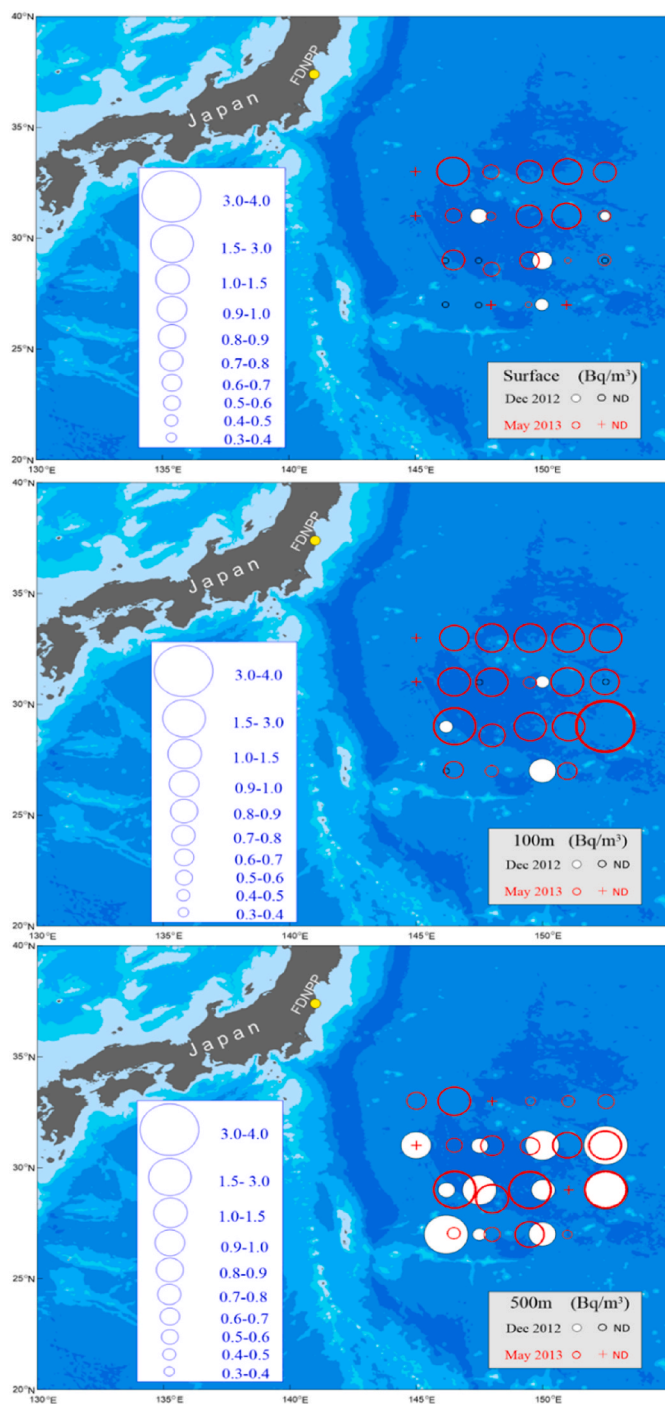
Fig. 2. Depths distribution of ^{134}Cs in 2012 and this study (2013) (surface, 100 m, 500 m). ^{134}Cs data in 2012 is cited from Deng et al.(2020). The red open circles denote the activities of radiocesium in 2013. The white solid circles denote the activities of radiocesium in 2012.The ND represents not detected or under the MDA.

Subtropical Mode Water (STMW). The study area is located at subtropical region, south of the Kuroshio extension. The FDNPP-derived radiocaesiums were transported eastward under the influence of the Kuroshio Extension and the Oyashio Current (Kumamoto et al., 2014; Men, 2021). Then part of FDNPP-derived radiocaesiums were trapped by STMW and CMW, subducted into the subsurface water and transported southwestward gradually from the formation area along the pycnocline of the ocean interior (25.0–25.6δ_θ for STMW and 26.0–26.6δ_θ for CMW, respectively) (Kaeriyama et al., 2014, 2016;

Aoyama et al., 2016a; Men et al., 2015; Kumamoto et al., 2013, 2014; Kaeriyama, 2017). As shown in Figure A2 and A3 in Appendix data, the distributions of subsurface ^{134}Cs activities correspond well to the STMW. Suga and Hanawa (1990) revealed that the STMW formation area is typically at 132–140°E north of 29°N, at 140-150°E north of 30°N, and at longitudes east of 150°E north of 31°N. Therefore, the surface activities of radiocesium decreased southward with the latitude.

However, the maximum activities of ^{134}Cs and ^{137}Cs at the depth of 100 m and 500 m were found at Station Q (29.01°N) and O (29°N) and the highest ^{137}Cs activities at the depth of 1000 m were also detected at these two stations. According to Cheng et al. (2014), the most active regions of eddies in the Northwest Pacific are the Kuroshio Extension region and the Subtropical Counter Current zone. And at the center of the western North Pacific Subtropical Gyre, it is also abundant in mesoscale eddies and submesoscale eddies (Qiu et al., 2014), where both Station Q and O were situated. Thus, it might be attributed to the mesoscale eddy. The sea level anomaly data derived from satellite altimetry are used to detecting the mesoscale eddies in the North Pacific (Cheng et al., 2014). As the sea surface height shown in Fig. 4, it indicates the presence of a cyclonic mesoscale eddy centered at ~28°N, 149.5°E, of which edge the Station Q and O located inside. Therefore, the convergence and subduction of surface water inside cyclonic eddy further promoted more radiocesiums downward transport and deeper penetration on the basis of the subduction of STMW. It was consistent with the conclusion reported in Budyansky et al. (2014) and Kumamoto et al. (2014).

Moreover, as exhibited in Fig. 5, the vertical distributions also reflect the same dynamic mechanism. The activities of radiocesiums at the depth of 100 m and 500 m were obviously higher than those in the surface layer (Table A2). Especially for the 100 m layer, the average and the maximum activities of radiocesiums at 100 m layer were significantly higher than those at the other two layers in this study. It is attributed that the Kuroshio Extension obstructed the transport of Fukushima-derived radiocesiums-enriched surface waters from its northern side to southern sides (Buesseler et al., 2012) on one hand and the North Pacific Mode Waters brought the Fukushima-derived radiocesiums into the ocean interior through the subsurface pathway on the other hand (Kaeriyama et al., 2014). Figs. 5–7 showed the vertical distributions of salinity (S), temperature (T), potential density (PD), ^{134}Cs, and ^{137}Cs for sections A-F, L-G, M-Q and R–U, respectively. The PDs of 25.0–25.6δ_θ and 26.0–26.6δ_θ were marked in yellow and pink color, respectively, which indicated the STMW and CMW (Kumamoto et al., 2013, 2014; Kaeriyama et al., 2014, 2016; Kaeriyama, 2017; Aoyama et al., 2016a; Men et al., 2015). As shown in Figs. 5 and 6, both STMW and CMW distributed in the upper 600 m layer (about 100~300 m for STMW and 400–600 m for CMW), which was corresponding to the ^{137}Cs and ^{134}Cs distributions (Fig. 7) at 100 m and 500 m layer, respectively. It confirmed further that the STMW and CMW transported the FDNPP-derived ^{137}Cs and ^{134}Cs to the subtropical region through the subsurface pathway, consistent with previous reports (Kumamoto et al., 2014; Kaeriyama et al., 2014). Especially, STMW transported more FDNPP-derived radiocesiums to the study area than CMW.

Besides, almost no FDNPP-derived ^{137}Cs and ^{134}Cs were detected at and below 1000 m layer and very few FDNPP-derived ^{137}Cs and ^{134}Cs were detected below 500 m. As shown in Figs. 5–7, the distributions of salinity, temperature, potential density suggested that the stratification occurred in the study area at the sampling time and there existed a low salinity water mass in the depth of ~500 m–700 m. The stratification and the low salinity water mass confined the water and the material exchange (nutrients, pollutants, etc.) between the upper water and the deeper water (Winn et al., 1995; Karl, 1999; Dore et al., 2002). In fact, the subtropical region where the sampling stations located is a typically oligotrophic marine desert. The surface waters in the North Pacific subtropical gyre are characterized by low nutrient and low biomass because of persistent thermal stratification (Dore et al., 2008). So strong vertical stratification in this study area occurs persistently. Therefore,
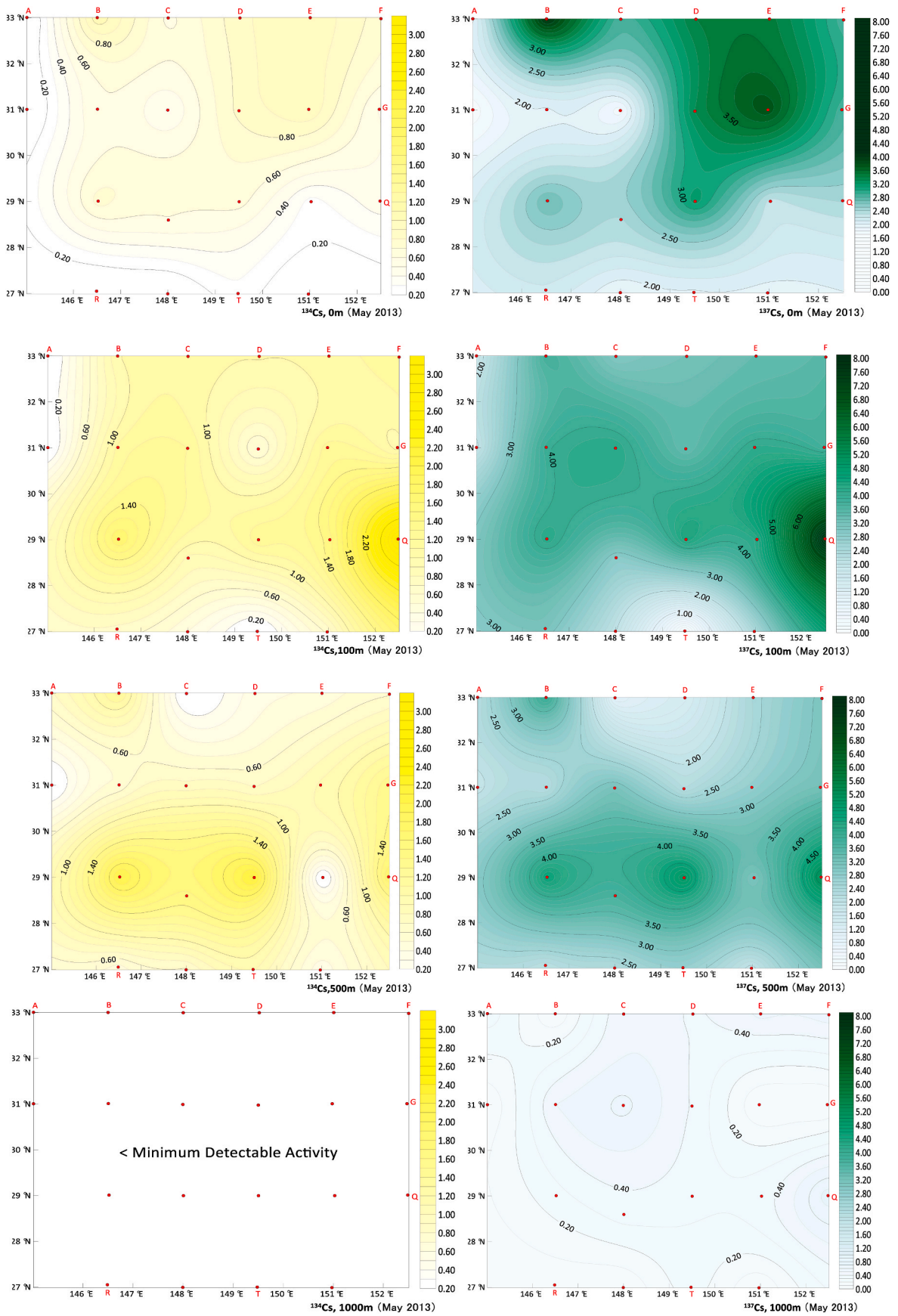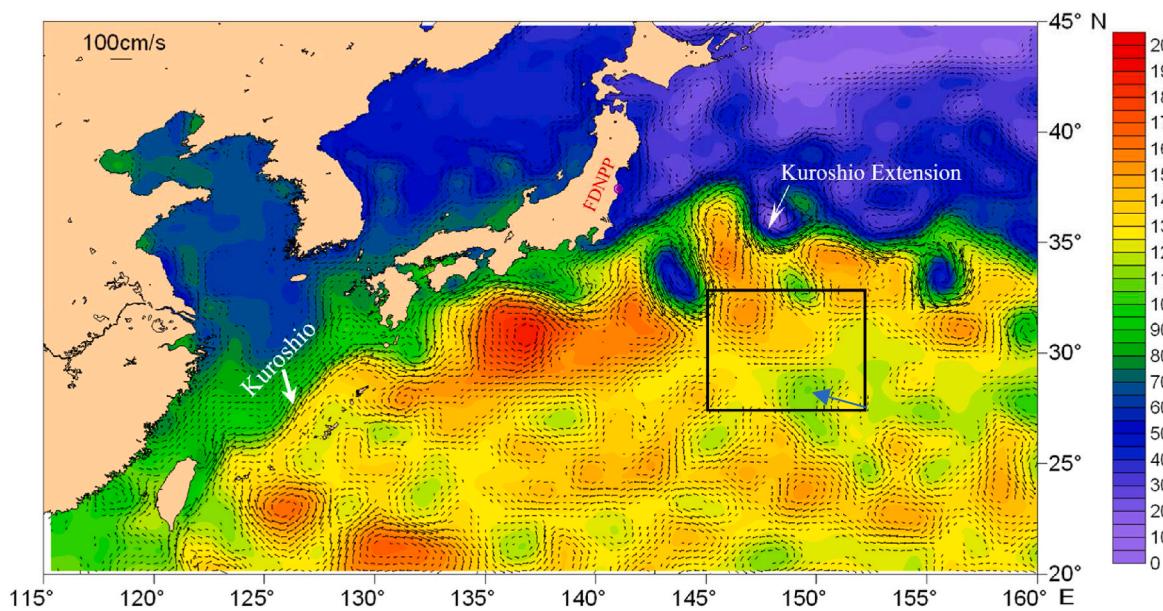
Fig. 3. Horizontal distributions of ^{137}Cs and [134]Cs at the different layers Red dots denote the Station U-,- respectively. Yellow represents the [134]Cs activity. Green represents the ^{137}Cs activity.

Fig. 4. Map of the average surface dynamic topography and geostrophic flows during April 24-June 2, 2013 The colors indicate the surface dynamic topography (cm). The white arrows indicate geostrophic flows. The red arrow denotes the cyclonic mesoscale eddy. Black square is the sampling area in this study.
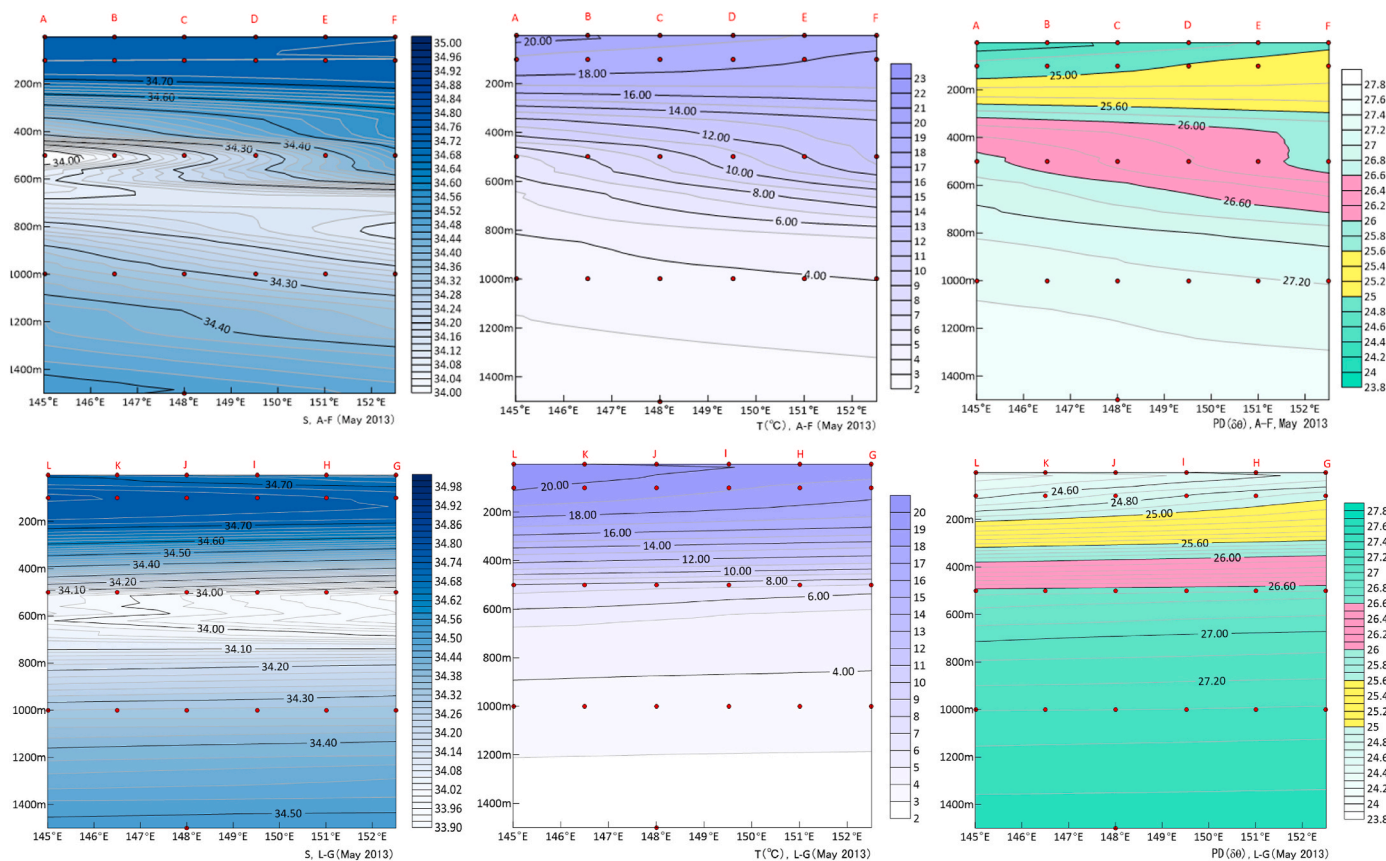
Fig. 5. The vertical distributions of salinity, temperature and potential density of sections A-F and L-G.

the FDNPP-derived ^{137}Cs and [134]Cs hardly penetrate to the deeper depth below 500 m layer, especially below 1000 m. According to the reason mentioned above, it was convinced that the transport of the mode waters along the subsurface pycnocline ($25.0–25.6\delta_\theta$ and $26.0–26.6\delta_\theta$) and the presence of vertical stratification as well as low salinity water mass resulted in the majority of the FDNPP-derived ^{137}Cs and [134]Cs

distributing in the upper 500 m of the water column.

4.4. Inventory of the radiocesiums in the study area

Based on the case that the majority of the ^{137}Cs and [134]Cs distributed in the upper 500 m of the water column, the water column inventories of
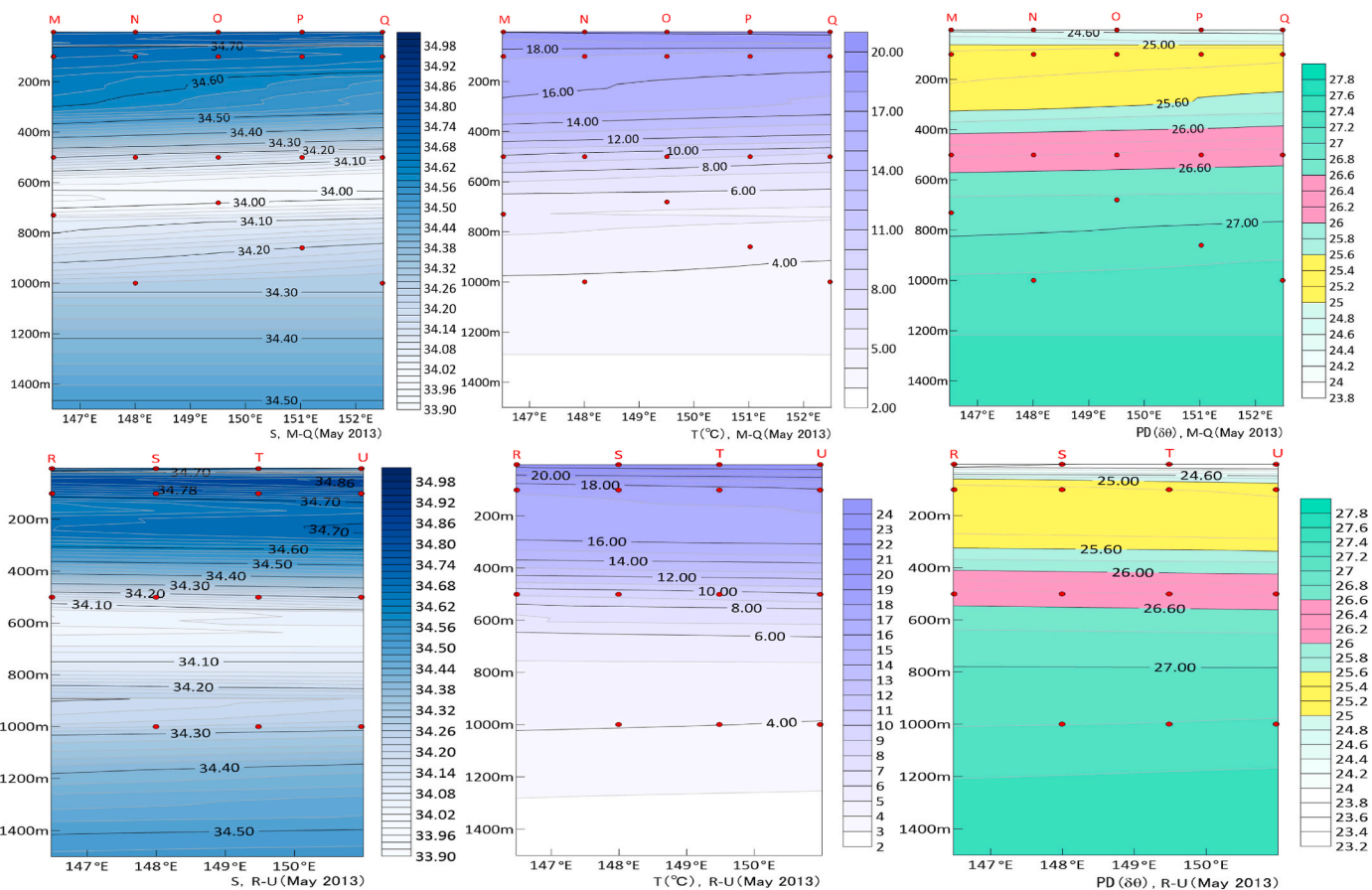
Fig. 6. The vertical distributions of salinity, temperature and potential density of sections M-Q and R–U.

^{137}Cs and ^{134}Cs in each station and the average inventory in the upper 500 m were estimated and listed in Table A3 in the Appendix data, according to the method in Ito et al. (2003). The average inventories of ^{137}Cs and ^{134}Cs were 1583 Bq/m^2 and 492 Bq/m^2. With the study area of 4.66×10^{11} m^2, it was estimated that the amounts of the ^{137}Cs (global and close-in fallout derived as well as FDNPP derived) and ^{134}Cs (FDNPP-derived) were 0.74 PBq and 0.23 PBq (P $= 10^{15}$), respectively. Base on the typical characteristic ratio, ^{134}Cs/^{137}Cs$_{activity\ ratio} \approx 1$ for FDNPP accident and decay correction of ^{134}Cs, the inventory of FDNPP-derived ^{137}Cs in the study area was estimated to be 0.46 PBq. According to Aoyama et al. (2016b), the inventory of ^{137}Cs released by FDNPP accident to the North Pacific Ocean was 15.5–18.5 PBq. Thus, the FDNPP-derived ^{137}Cs in the study area accounts for 2.5–3.0% of the total ^{137}Cs released by FDNPP to the North Pacific Ocean. The inventory of ^{137}Cs from global and close-in fallout was calculated to be 0.28 PBq (0.74 minus 0.46). Therefore, at the sampling time, May of 2013, FDNPP accident elevated the inventory of ^{137}Cs in the study area ~1.6 times higher than ever.

5. Conclusion

In this study, the distributions of ^{137}Cs and ^{134}Cs in the seawater of subtropical area in May 2013 were determined. The highest ^{137}Cs and ^{134}Cs activities were 7.88 Bq/m^3 and 3.40 Bq/m^3, respectively. No FDNPP-derived Cs was found below 1000 m layer of the water column in the Subtropical area. The FDNPP accident contributed 0.46 PBq of ^{137}Cs to the upper 500 m of water column, which was ~1.6 times of the background amount (0.28 PBq). The surface activities of ^{137}Cs and ^{134}Cs activities at each longitude decreased southward gradually with the latitude from 33°N to 26°N. The significant increase in ^{137}Cs and ^{134}Cs activities in 100 m layer was mainly attributed to the STMW which

carried ^{137}Cs and ^{134}Cs along the subsurface isopycnals (25.0–25.6 δ_θ) at the depth of ~100 m–~300 m to the subtropical region. As time went on, more FDNPP-derived radiocesiums were transported to the south of the KE. And more FDNPP-derived radiocesiums were subducted to the subsurface layer and deeper layer by STMW than ever. The cyclonic eddy further promoted more radiocesiums downward transport and deeper penetration on the basis of the subduction of STMW.

However, the hard penetration of FDNPP-derived ^{137}Cs and ^{134}Cs to the deeper depth below 500 m layer, especially below 1000 m was associated with the formation of vertical stratification as well as the presence of low salinity water mass.

Credit author statement

Fenfen Wang: Investigation, sample and data analysis, writing original draft preparation, reviewing and editing. **Wu Men**: Investigation, designation, methodology, writing-reviewing and editing. **Jiang Huang**: Investigation. **Zhaohui Chen**: Physical oceanography analysis. **Lixiao Xu**: Physical oceanography analysis.

Competing financial interests

The authors declare no competing financial interest.

Declaration of competing interest

The authors declare that they have no known competing financial interests or personal relationships that could have appeared to influence the work reported in this paper.
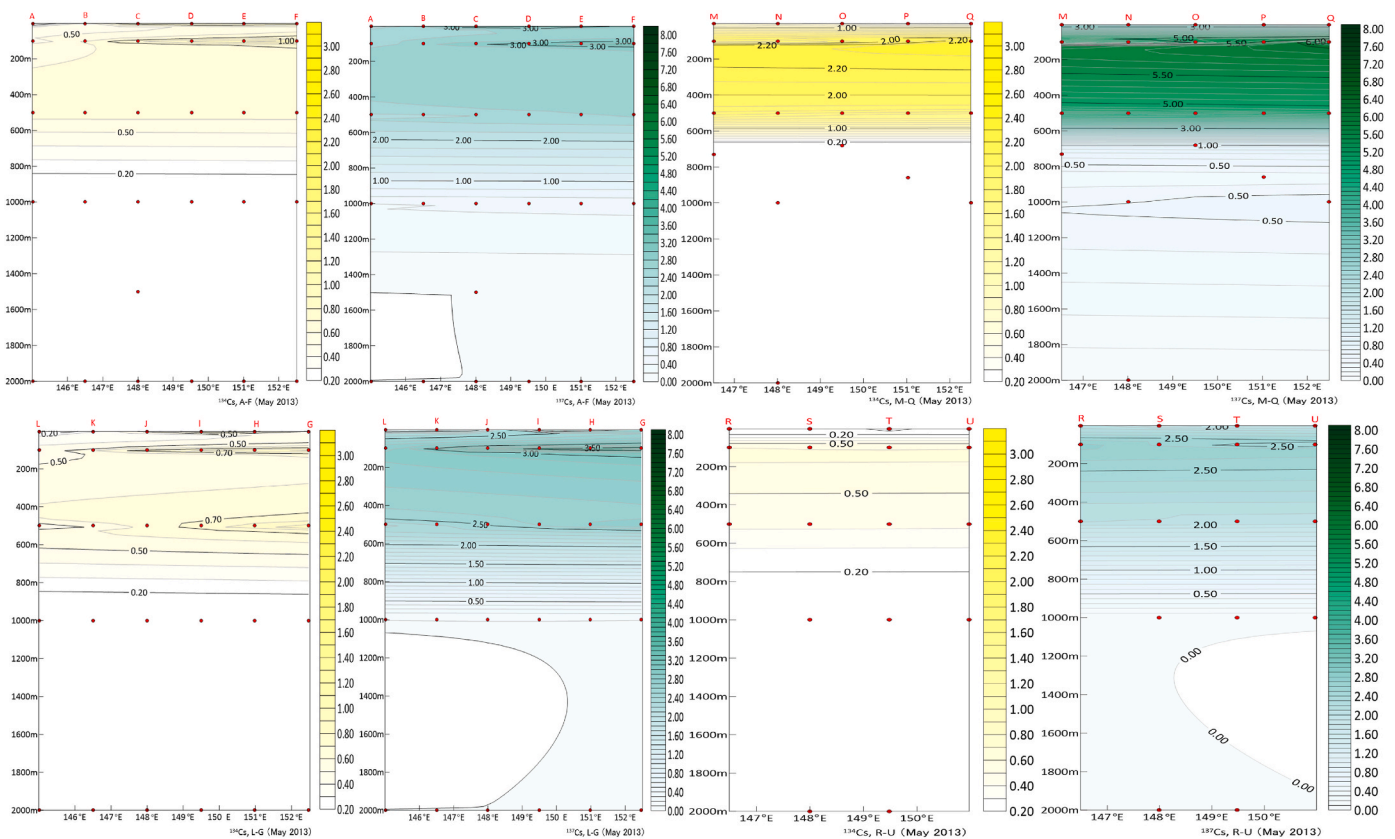
Fig. 7. The vertical distributions of ^{134}Cs and ^{137}Cs in sections A-F, L-G, M -Q and R–U.

Data availability

Data will be made available on request.

Acknowledgements

Appendix A. Supplementary data

Supplementary data to this article can be found online at https://doi.org/10.1016/j.chemosphere.2023.139314.

References

Aoyama, M., Hamajima, Y., Hult, M., Uematsu, M., Oka, E., Tsumune, D., Kumamoto, Y., 2016a. ^{134}Cs and ^{137}Cs in the North Pacific Ocean derived from the TEPCO Fukushima Dai-ichi nuclear power plant accident, Japan in march 2011: part one- surface pathway and vertical distributions. J. Oceanogr. 72, 53–65.

Aoyama, M., Kajino, M., Tanaka, T.Y., Sekiyama, T.T., Tsumune, D., Tsubono, T., Hamajima, Y., Inomata, Y., Gamo, Y., 2016b. ^{134}Cs and ^{137}Cs in the North Pacific Ocean derived from the TEPCO fukushima dai-ichi nuclear power plant accident, Japan in march 2011: part two – estimation of ^{134}Cs and ^{137}Cs inventories in the North Pacific Ocean. J. Oceanogr. 72, 67–76.

Aoyama, M., Tsumune, D., Hamajima, Y., 2013a. Distribution of ^{137}Cs and ^{134}Cs in the North Pacific Ocean: impacts of the TEPCO fukushima-daiichi NPP accident. J. Radioanal. Nucl. Chem. 296, 535–539.

Aoyama, M., Uematsu, M., Tsumune, D., Hamajima, Y., 2013b. Surface pathway of radioactive plume of TEPCO Fukushima NPP1 released ^{134}Cs and ^{137}Cs. Biogeosciences 10, 3067–3078.

Budyansky, M.V., Goryachev, V.A., Kaplunenko, D.D., Lobanov, V.B., Prants, S.V., Sergeev, A.F., Shlyk, N.V., Uleysky, M.Yu, 2014. Role of mesoscale eddies in transport of Fukushima-derived cesium isotopes in the ocean. Deep-Sea Res. I 96, 15–27.

Buesseler, K., Dai, M., Aoyama, M., Benitez-Nelson, C., Charmasson, S., Higley, K., Maderich, V., Masque, P., Morris, P.J., Oughton, D., Smith, J.N., 2017. Fukushima daiichi derived radionuclides in the ocean: transport, fate, and impacts. Ann. Rev. Mar. Sci 9, 173–203.

Buesseler, K.O., Jayne, S.R., Fisher, N.S., Rypina, I.I., Baumann, H., Baumann, Z., et al., 2012. Fukushima-derived radionuclides in the ocean and biota off Japan. Proc. Natl. Acad. Sci. USA 109, 5984–5988.

Buesseler, K.O., 2014. Fukushima and ocean radioactivity. Oceanography 27 (1), 92–105.

Cheng, Y.H., Ho, C.R., Zheng, Q., Kuo, N.J., 2014. Statistical characteristics of mesoscale eddies in the North pacific derived from satellite altimetry. Rem. Sens. 6, 5164–5183.

Christoudias, T., Lelieveld, J., 2013. Modelling the global atmospheric transport and deposition of radionuclides from the Fukushima Dai-ichi nuclear accident. Atmos. Chem. Phys. 13, 1425–1438.

Deng, F., Lin, F., Yu, W., He, J., Wang, F., Chen, Z., 2020. The distributions of ^{134}Cs, ^{137}Cs and ^{90}Sr in the northwest Pacific seawater in the winter of 2012. Mar. Pollut. Bull. 152, 1109000.

Dore, J.E., Brum, J.R., Tupas, L.M., Karl, D.M., 2002. Seasonal and interannual variability in sources of nitrogen supporting export in the oligotrophic subtropical North Pacific Ocean. Limnol. Oceanogr. 47, 1595–1607.

Dore, J.E., Letelier, R.M., Church, M.J., Lukas, R., Karl, D.M., 2008. Summer phytoplankton blooms in the oligotrophic North Pacific Subtropical Gyre: historical perspective and recent observations. Prog. Oceanogr. 76, 2–38.

Hanawa, K., Yoritaka, H., 2001. North Pacific Subtropical Mode Waters observed in long XBT cross sections along 32.5°N line. J. Oceanogr. 57, 679–692.

Inoue, M., Kofuji, H., Hamajima, Y., Nagao, S., Yoshida, K., Yamamoto, M., 2012. ^{134}Cs and ^{137}Cs activities in coastal seawater along northern sanriku and tsugaru strait, northeastern Japan, after fukushima dai-ichi nuclear power plant accident. Environ. Radioactiv. 111, 116–119.

Inomata, I., Aoyama, M., Tsubono, T., Tsumune, D., Kumamoto, Y., Nagai, H., Yamagata, T., Kajino, M., Tanaka, Y.T., Sekiyama, T.T., Oka, E., Yamada, M., 2018. Estimate of fukushima-derived radiocaesium in the North Pacific Ocean in summer 2012. J. Radioanal. Nucl. Chem. 318, 1587–1596.

Ito, T., Aramaki, T., Kitamura, T., Otosaka, S., Suzuki, T., Togawa, O., Kobayashi, T., Senjyu, T., Chaykovskaya, E.L., Karasev, E.V., Lishavskaya, T.S., Novichkov, V.P.,

Tkalin, A.V., Shcherbinin, A.F., Volkov, Y.N., 2003. Anthropogenic radionuclides in the Japan Sea: their distributions and transport processes. J. Environ. Radioact. 68, 249–267.

Kaeriyama, H., 2017. Oceanic dispersion of Fukushima-derived radioactive cesium:a review. Fish. Oceanogr. 26, 99–113.

Kaeriyama, H., Shimizu, Y., Setou, T., Kumamoto, Y., Okazaki, M., Ambe, D., Ono, T., 2016. Intrusion of Fukushima-derived radiocaesium into subsurface water due to formation of mode waters in the North Pacific. Sci. Rep. 6, 22010–22020.

Kaeriyama, H., Shimzu, Y., Ambe, D., Masujima, M., Shigenobu, Y., Fujimoto, K., Ono, T., Nishiuchi, K., Taneda, T., Kurogi, H., Setou, T., Sugisaki, H., Ichikawa, T., Hidaka, K., Hiroe, Y., Kusaka, A., Kodama, T., Kuriyama, M., Morita, H., Nakata, K., Morinaga, K., Morita, T., Watanabe, T., 2014. Southwest intrusion of ^{134}Cs and ^{137}Cs derived from the fukushima dai-ichi nuclear power plant accident in the western North Pacific. Environ. Sci. Technol. 45, 3120–3127.

Karl, D.M., 1999. A sea of change: biogeochemical variability in the North Pacific subtropical gyre. Ecosystems 2, 181–214.

Kumamoto, Y., Aoyama, M., Hamajima, Y., Aono, T., Kouketsu, S., Murata, A., Kawano, T., 2014. Southward spreading of the fukushima-derived radiocaesium across the Kuroshio extension in the North pacific. Sci. Rep. 4, 4276.

Kumamoto, Y., Aoyama, M., Hamajima, Y., Murata, A., Kawano, T., 2015. Impact of the Fukushima-derived radiocesium in the western North Pacific Ocean about ten months after the Fukushima Dai-ichi nuclear power plant accident. J. Environ. Radioact. 140, 114–122.

Kumamoto, Y., Murata, A., Kawano, T., Aoyama, M., 2013. Fukushima-derived radiocaesium in the northwestern Pacific Ocean in february 2012. Appl. Radiat. Isot. 81, 335–339.

Kumamoto, Y., Yamada, M., Aoyama, M., Hamajima, Y., Kaeriyama, H., Nagai, H., Yamagata, T., Murata, A., Masumoto, Y., 2019. Radiocaesium in north pacific coastal and offshore areas of Japan within several months after the fukushima accident. J. Environ. Radioact. 198, 79–88.

Lin, W., Chen, L., Yu, W., Ma, H., Zeng, Z., Lin, J., Zeng, S., 2015. Radioactivity impacts of the Fukushima nuclear accident on the atmosphere. Atmos. Environ. 102, 311–322.

Men, W., He, J., Wang, F., Yu, W., Li, Y., Huang, J., Yu, X., 2015. Radioactive status of seawater in the northwest Pacific more than one year after the Fukushima nuclear accident. Sci. Rep. 5, 7757.

Men, W., 2021. Discharge of contaminated water from the fukushima daiichi nuclear power plant accident into the Northwest pacific: what is known and what needs to be known. Mar. Pollut. Bull., 112984

Nakata, K., Sugisaki, H., 2015. Impacts of the Fukushima Nuclear Accident on Fish and Fishing Grounds. Springer Japan eBook, p. 238, 978-4-431-55537-7.

Qiu, B., Chen, S.M., Klein, P., Sasaki, H., Sasai, Y., 2014. Seasonal mesoscale and submesoscale eddy variability along the North pacific subtropical countercurrent. J. Phys. Oceaogr. 44, 3079–3098.

Suga, T., Hanawa, K., 1990. The mixed-layer climatology in the northwestern part of the North Pacific subtropical gyre and the formation area of Subtropical Mode Water. J. Mar. Res. 48, 543–566.

Takata, H., Kusakabe, M., Inatomi, N., Ikenoue, T., 2018. Appearances of fukushima daiichi nuclear power plant-derived ^{137}Cs in coastal waters around Japan: results from marine monitoring off nuclear power plants and facilities, 1983–2016. Environ. Sci. Technol. 52, 2629–2637.

METI (Ministry of Economy, Trade and Industry), 2022. Mid-and-Long-Term Roadmap towards the Decommissioning of TEPCO's Fukushima Daiichi Nuclear Power Station. Units 1-4. https://www.meti.go.jp/english/earthquake/nuclear/decommissioning/pdf/1f_status_20220307.pdf.

Wang, F., Men, W., Yu, T., Huang, J., He, J., Lin, F., Deng, F., 2022a. Intrusion of fukushima-derived radiocesium into the east China sea and the northeast south China sea in 2011–2015. Chemosphere 294, 133546.

Wang, F., Men, W., Huang, J., Yu, T., He, J., Yu, W., Li, Y., 2022b. Fukushima-derived radiocesium in the waters of the Northwest Pacific ocean in the winter of 2011. Mar. Pollut. Bull. 176, 113465.

Winn, C.D., Campbell, L., Christian, J.R., Letelier, R.M., Hebel, D.V., Dore, J.E., Fujieki, L., Karl, D.M., 1995. Seasonal variability in the phytoplankton community of the North pacific subtropical gyre. Global Biogeochem. Cycles 9, 605–620.

Yoshida, N., Kanda, J., 2012. Tracking the fukushima radionuclides. Science 336, 1115–1116. https://doi.org/10.1126/science.1219493.

TEPCO (Tokyo Electric Power Company). 2021. The Handling ALPS Treated Water, https://www.tepco.co.jp/en/decommission/progress/watertreatment/oceanrelease/index-e.html.